

**Microplasticity in a precipitation hardening Al-Cu-Si-Mg alloy**

The variation of the hardness of a complex aluminium precipitation hardening alloy (L70 type), of composition Al-4 wt% Cu-0.8 wt% Si-0.8 wt% Mg-0.7 wt% Mn-0.5 wt% Fe, with ageing times at room temperature, 130, 160 and 190°C, has been correlated previously [1,2] with transmission electron microscope observations of precipitate morphology. It was established that the peak hardness after both 160 and 190°C ageing was associated with coherent  $\theta'$  particles and that the subsequent limited over-ageing at these temperatures was controlled by the slow growth of  $\theta'$  particles. In contrast, ageing at 130°C gave a series of hardness plateaux, which were attributed to the sequential precipitation of GPI zones,  $\theta''$  and  $\theta'$  precipitates. In addition, at 130°C, there was evidence for the formation of some complex zones of the GPB type (Al-

Cu-Si-Mg) during the initial stages of ageing, while the hardening noted at room temperature appeared almost entirely dependent on GPB zone formation. In this note, the microstrain characteristics of aluminium L70 alloy are reported for a range of dislocation and precipitate substructures, with reference to the microscopic yield stress (MYS) (the stress to produce a plastic strain of  $2 \times 10^{-6}$ ) and the friction stress,  $\sigma_F$ , (the stress for the initiation of anelastic deformation).

The alloy investigated was commercial aluminium L70, with composition as given above. Most specimens were solution treated (500°C for 2 h and water quenched) and then aged at room temperature, 130 or 190°C, while some specimens were 1.5% cold worked after solution treatment and then aged at room temperature. All specimens were of rectangular cross section and were electropolished prior to tensile testing [3,4] at room temperature.

The room temperature microstrain properties

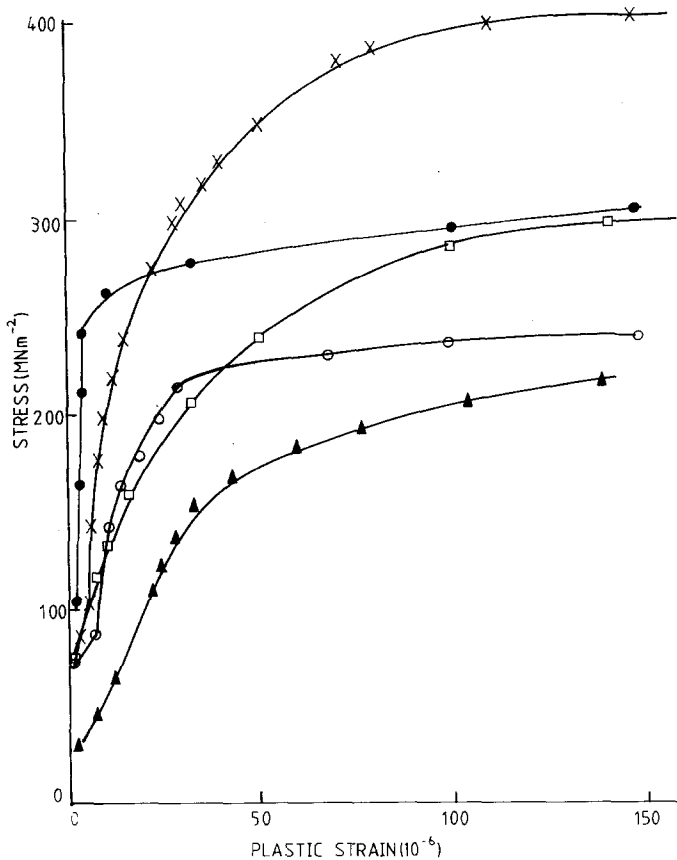


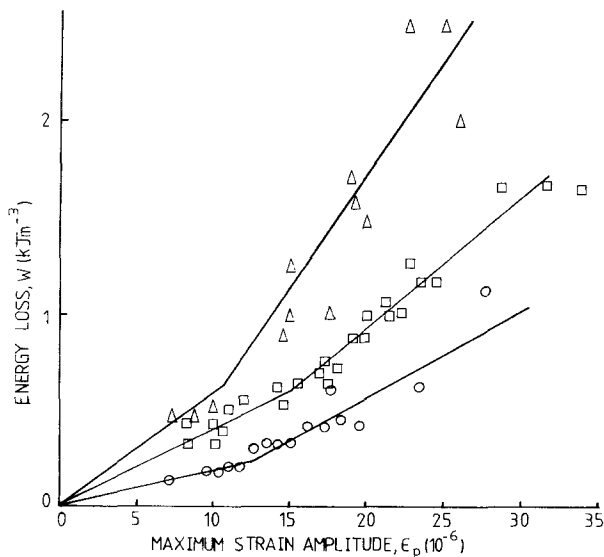
Figure 1 Stress-plastic strain curves in the microstrain region for: ▲ ST, aged at 190°C for 504 h; ○ ST, aged at room temperature for > 48 h; ◻ ST, aged at 190°C for 72 h; ● ST, 1.5% CW, aged at room temperature for > 48 h and × ST, aged at 190°C for 9 h.

were determined with both a Tuckerman optical strain gauge and a capacitance gauge [4]. A load-unload technique was used to determine the friction stress,  $\sigma_F$ , the microscopic yield stress (MYS) and the stress-plastic strain curve in the microstrain region. A step loading technique was employed with the optical gauge, while continuous load-unload cycles were obtained with the capacitance gauge.

The MYS for a particular ageing condition was determined directly from the associated experimental stress-plastic strain curve, (with some typical curves shown in Fig. 1). The stress to produce  $100 \times 10^{-6}$  plastic strain,  $\sigma_m$ , was also determined as a measure of the onset of macroscopic flow or "gross microyielding" [5]. In contrast,  $\sigma_F$  was derived from the closed stress-total strain hysteresis loops obtained at stress levels below the MYS [5], with the energy dissipated per loop,  $W$ , given by the loop area, related to the strain amplitude,  $\epsilon_p$ , represented by the maximum loop width, by the equation [6]

$$\sigma_F = \frac{W}{2\epsilon_p} \quad (1)$$

$(W - \epsilon_p)$  curves were determined for some of the ageing conditions, as shown in Fig. 2, which reveals that the  $(W - \epsilon_p)$  variation can be represented by two linear slopes, as has also been found in previous work on various metals and alloys (e.g. [5]).



As Equation 1 is applicable in the limit as  $\epsilon_p \rightarrow 0$ , then values of  $\sigma_F$  were taken from the initial slope. This slope was not affected by pre-straining the test specimens, which only served to increase the extent of the second linear slope, but with the limited data obtained, the values of  $\sigma_F$  obtained should be considered as approximations.

Table I lists the various ageing conditions investigated and details the corresponding microstructures, MYS,  $\sigma_F$  and hardness values. It should be noted that, as the alloy aged at room temperature, it was not possible to determine the microstrain properties of the as-quenched condition and the microstrain properties reached an approximate constant, "equilibrium" level, after an ageing time of  $\sim 48$  h.

From Table I, it is interesting to note that ageing to the maximum hardness does not necessarily produce a corresponding maximum in the MYS. In fact, the maximum MYS measured is associated with the "under-aged" condition achieved by room-temperature ageing. This maximum value of MYS developed by room-temperature ageing from the solution treated plus 1.5% cold work condition, is attributed to the presence of a high density of GPB zones ( $\sim 10^{16} \text{ m}^{-2}$ ) [3]. It appears that the MYS depends on the density of GPB zones, as the smaller value of MYS obtained after room-temperature ageing from the solution treated condition (without cold work) is associated with a lower density of GPB zones ( $\sim 10^{13} \text{ m}^{-2}$ ) [3].

Figure 2 Energy loss ( $W$ ) plotted against maximum strain amplitude  $\epsilon_p$  from closed hysteresis loops, with  $\Delta$  representing solution treated and solution treated with 1.5% cold worked specimens aged at room temperature for  $> 48$  h (with prestrains up to  $1.2 \times 10^{-2}$ ),  $\square$  representing solution treated specimens aged at  $190^\circ\text{C}$  for 72 h (with prestrains up to  $2.0 \times 10^{-2}$ ) and  $\circ$  representing solution treated specimens aged at  $190^\circ\text{C}$  for 504 h (with prestrains up to  $8.4 \times 10^{-3}$ ).

TABLE I Microstrain properties of Al L70 alloy

Starting condition	Ageing temperature (° C)	Ageing time (h)	Hardness (VHN)	Microstructure	MYS at $2 \times 10^{-6}$ (MN m <sup>-2</sup> )	$\sigma_F$ (MN m <sup>-2</sup> )	$\sigma_m$ at $100 \times 10^{-6}$ (MN m <sup>-2</sup> )
ST	RT	48–240	133	GPBZ	75	20	240
ST 1.5% CW	RT	48–240	130	GPBZ	105	20	300
ST	130	7	122	GPI/GPBZ	56	–	148
ST	130	20	128	GPI/GPBZ	50	–	166
ST	130	40	133	GPBZ	78	–	170
ST	130	80	151	$\theta''$	70	–	216
ST	130	150	162	$\theta'$	100	–	300
ST	190	2	158	GPI/ $\theta''$	92	–	360
ST	190	4.5	162	$\theta'$	62	–	390
ST	190	9	162	$\theta'$	72	–	460
ST	190	72	130	$\theta'$	72	29	290
ST	190	150	120	$\theta'$	65	–	250
ST	190	504	118	$\theta'$	32	9	200

ST – Solution treated.

ST 1.5% CW – Solution treated and 1.5% cold worked.

The dependence of MYS on the density of zones is also illustrated by the progressive increase in MYS during 130° C ageing for times up to 40 h, during which the density of zones is also increasing. In this case a mixture of GPI and GPB zones are obtained [2], with the GPB zones having a different composition of those created during room-temperature ageing [2]. However, it can be seen from Table I that these differences do not effect the MYS, as the values obtained from the solution treated condition are similar for room-temperature and 130° C ageing. With continued ageing from 40 h at 130° C, the MYS increased as the transformation from zones to  $\theta''$  and  $\theta'$  precipitate proceeded, with the maximum MYS at this ageing temperature associated with the presence of coherent  $\theta'$  precipitate. Ageing at 190° C gave an initial high MYS associated with a GPI/ $\theta''$  structure, but the significant characteristic is the relatively constant value of MYS for ageing times from 4.5 to 150 h, during which a progressive but slow, coarsening of  $\theta'$  particles occurs [1] with a corresponding reduction in the number of  $\theta'$  particles. Hence it appears that the MYS is not critically dependent on the density of  $\theta'$  particles. The significant decrease in MYS after 504 h at 130° C coincides with the transition from coherent to non-coherent  $\theta'$  particles [2]. It appears that  $\sigma_F$  also decreases significantly for this condition, although the limited  $\sigma_F$  data obtained does not yet allow a distinction between the possible contri-

butions of the loss of coherency and the depletion of the matrix solid solution.

### Acknowledgements

The provision of an equipment and maintenance grant (PKD) for this research by the Ministry of Defence (PE) is gratefully acknowledged, together with the support of Mr C. R. Milne and Mr M. Trapaud of the Royal Aircraft Establishment.

### References

1. W. BONFIELD and P. K. DATTA, *J. Mater. Sci.* **11** (1976) 1661.
2. *Idem, ibid.* **12** (1977) 1050.
3. P. K. DATTA, Ph.D. Thesis, University of London, 1974.
4. W. BONFIELD, P. K. DATTA, B. C. EDWARDS and D. C. PLANE, *J. Mater. Sci.* **8** (1973) 1832.
5. W. BONFIELD and B. C. EDWARDS, *ibid.* **10** (1975) 492.
6. P. LUKAS and M. KLESNIL, *Phys. Stat. Sol.* **11** (1965) 127.

Received 20 March  
and accepted 2 April 1980

W. BONFIELD  
Department of Materials,  
Queen Mary College,  
London E1 4NS, UK

P. K. DATTA  
Department of Materials Science,  
Newcastle Polytechnic,  
Newcastle upon Tyne, UK